Hindawi
Journal of Diabetes Research
Volume 2022, Article ID 3025538, 15 pages
https://doi.org/10.1155/2022/3025538

Research Article

Improvement of Lipotoxicity-Induced Islet β Cellular Insulin Secretion Disorder by Osteocalcin

Yafang Zhang,[1] **Ling Li**,[1] **Yongze Zhang**,[1,2,3] **Sunjie Yan**,[1,2,3] **and Lingning Huang**[1,2,3]

[1]*Department of Endocrinology, The First Affiliated Hospital of Fujian Medical University, No 20 Chazhong Road, Fuzhou, 350004 Fujian province, China*
[2]*Diabetes Research Institute of Fujian Province, No 20 Chazhong Road, Fuzhou, 350004 Fujian province, China*
[3]*Institute of Metabolic Diseases of Fujian Medical University, No 20 Chazhong Road, Fuzhou, 350004 Fujian province, China*

Correspondence should be addressed to Lingning Huang; hlnlily@fjmu.edu.cn

Received 17 August 2021; Revised 10 November 2021; Accepted 26 February 2022; Published 12 March 2022

Academic Editor: Riccardo Calafiore

Background. Osteocalcin (OCN) has been proved to be closely related with the development of type 2 diabetes mellitus (T2DM). We aimed to study if OCN could improve the disorder of islet cell caused by lipotoxicity. *Methods.* Alizarin red staining was used to investigate the mineralization. Western blotting and ELISA methods were used to measure protein expression. Immunofluorescence staining was used to investigate the protein nuclear transfer. *Results.* High glucose and high fat inhibited the differentiation of osteoblast precursors. Overexpression of insulin receptor ($InsR^{OE}$) significantly promoted the Runx2 and OCN expression. The increase of insulin, Gprc6a, and Glut2 by osteoblast culture medium overexpressing insulin receptor was reversed by osteocalcin neutralizing antibody. Undercarboxylated osteocalcin (ucOC) suppressed the lipotoxic islet β-cell damage caused by palmitic acid. The FOXO1 from intranuclear to extranuclear was also significantly increased after ucOC treatment compared with the group PA. Knockdown of Gprc6a or suppression of PI3K/AKT signal pathway could reverse the upregulation of GPRC6A/PI3K/AKT/FoxO1/Pdx1 caused by ucOC. *Conclusion.* OCN could activate the FOXO1 signaling pathway to regulate GLUT2 expression and improve the insulin secretion disorder caused by lipotoxicity.

1. Introduction

Type 2 diabetes mellitus (T2DM) is one of the most common diseases threatening human health [1, 2], and its pathogenesis is complex. The insulin synthesis, processing, secretion disorders, and insulin resistance are the main pathological mechanisms associated with the β-cell dysfunction [3]. The pancreatic β-cell dysfunction is a focus clinical indication of diabetes by impairing the ability of insulin secretion [4, 5]. Additionally, the lipotoxicity was an indispensable factor modulated by inflammatory mediators and cytokines [6, 7]. It was reported that the lipotoxicity could directly activate the TLR4-JNK pathway cascade in islet β-cells and further induce insulin secretion disorder and β-cell apoptosis [8]. The oxidative stress, endoplasmic reticulum stress, and inflammation can also lead to dedifferentiation of mature β-cells, which is an important factor in functional cell reduction and insulin secretion deficiency in diabetes patients [9, 10]. In addition, chronic exposure to high concentrations of saturated fatty acids, such as palmitic acid (PA), could lead to apoptosis of pancreatic β-cells [11–13].

Osteocalcin (OCN) is the bridge between bone metabolism and energy metabolism [13]. After entering the blood circulation, it decarboxylates under the action of vitamin K-related enzymes and exists in the blood circulation in the form of carboxylated incomplete OCN [14, 15]. Some researchers found that there was no abnormal bone metabolism after selective OCN gene knockout in rats [16]. However, fat thickness, insulin level, glucose tolerance, and other metabolic indicators could be changed [17–19]. Meanwhile, OCN may regulate energy metabolism and have

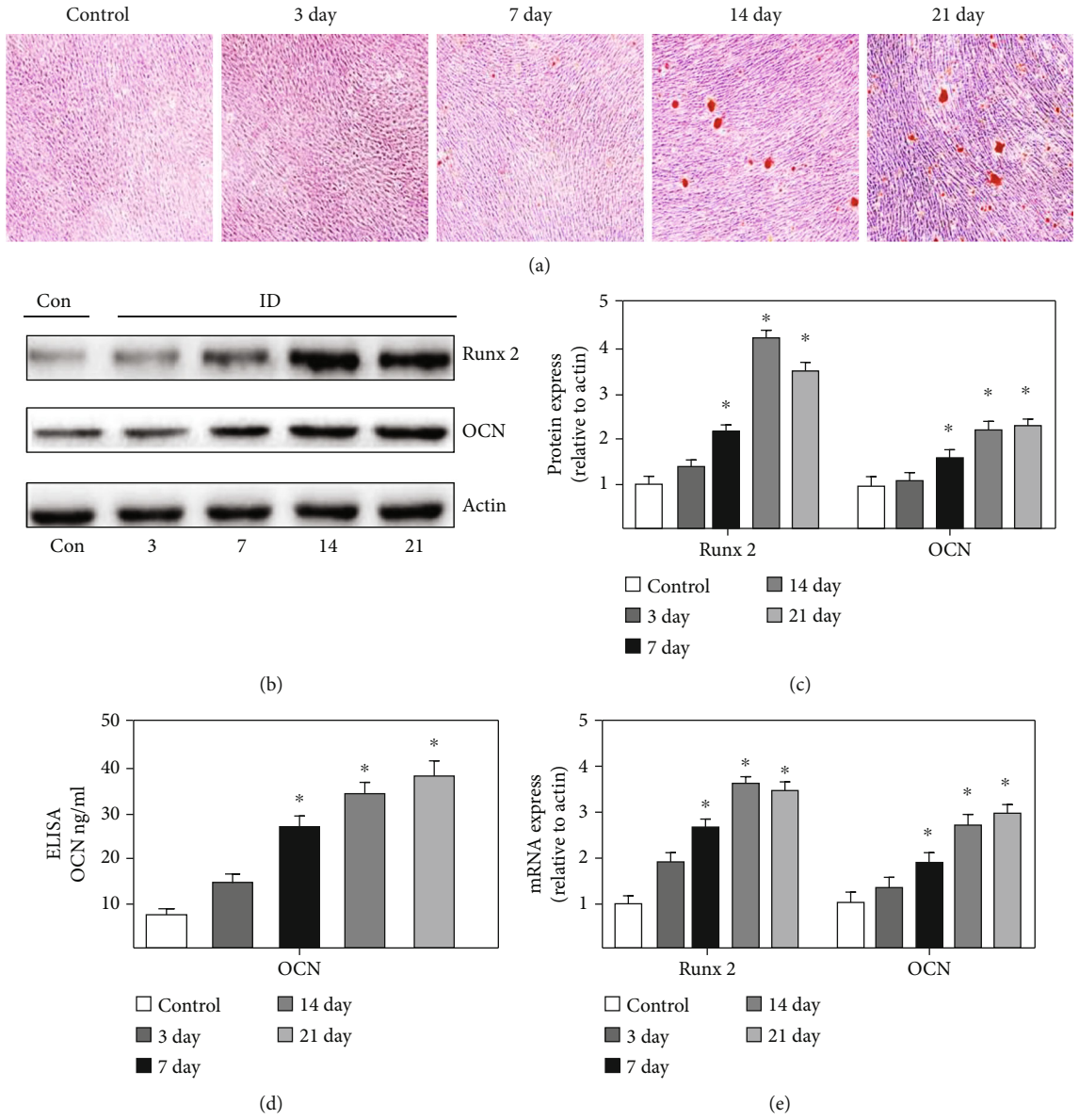

Figure 1: Induction time of osteogenic precursor cells. (a) Mineralization was analyzed through alizarin red staining. (b) The protein expression of Runx2 and OCN was measured through western blotting. (c) The protein expression of Runx2 and OCN was analyzed. (d) The level of OCN was measure with ELISA. (e) The mRNA expression of Runx2 and OCN was detected. Compared with the control group, $^{*}P < 0.05$. MC3T3-E1 was used in these experiments.

endocrine activity [16, 20, 21]. After intervention with exogenous OCN, the fat thickness of mice fed with high fat and high glucose was decreased, but the insulin secretion and sensitivity were increased [22–25]. Previous study showed that OCN treatment improved glucose homeostasis and lipid metabolism [26]. These evidences indicate that OCN may improve T2DM and glucose and lipid metabolism disorders, but the specific mechanism remains unclear.

Some studies have confirmed that OCN can stimulate insulin secretion [27]. In addition, the serum level of OCN in patients with T2DM was reduced [28]. This may further reduce insulin secretion and aggravate the progression of T2DM. However, the specific mechanism of OCN in insulin synthesis and secretion remains unclear. These evidences prove that bone metabolism and glucose metabolism may form endocrine rings and interfere with each other. OCN may become a new target for the treatment of metabolic diseases.

2. Materials and Methods

2.1. Cell Culture. The MC3T3-E1 cell line was purchased from American Type Culture Collection (ATCC, Manassas, VA, USA). Cells were incubated with a-MEM (Gibco, USA) containing 1% penicillin-streptomycin and 10% heat-inactivated fetal bovine serum (FBS) at 37°C with 5% CO_2. β-TC6 cell line purchased from ATCC was cultured with DMEM containing 10 mmol/L HEPES, 2 mmol/L L-

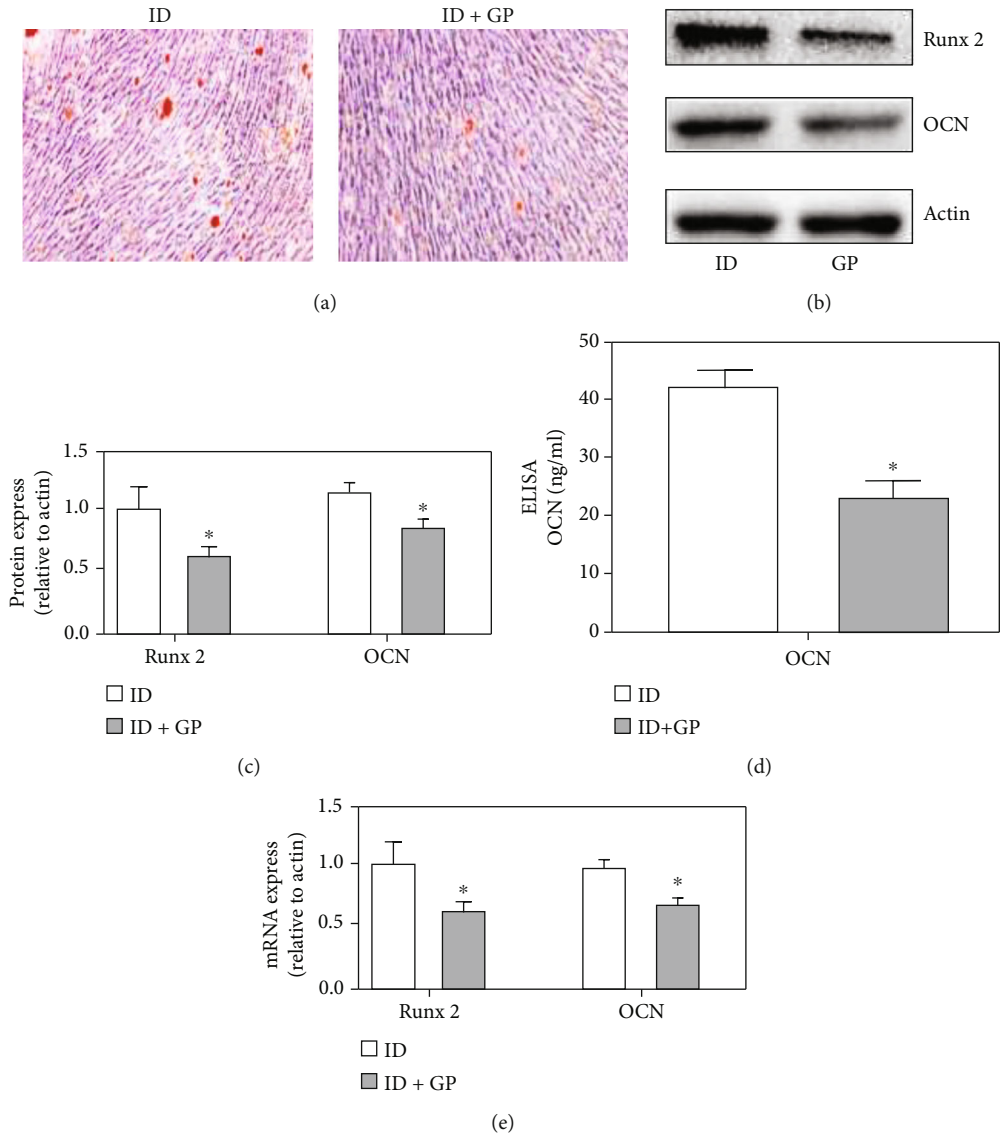

Figure 2: High glucose and high fat inhibited the differentiation of osteoblast precursors. (a) Mineralization was analyzed through alizarin red staining. (b) The protein expression of Runx2 and OCN was measured through western blotting after treatment with ID or ID+GP; (c) The protein expression of Runx2 and OCN was analyzed. (d) The level of OCN was measured with ELISA. (e) The mRNA expression of Runx2 and OCN was detected. Compared with the ID group, $^*P < 0.05$. MC3T3-E1 was used in these experiments.

glutamine, 10% FBS, and 25 mmol/L glucoses on the condition of 95% air and 5% CO_2 at 37°C.

2.2. Cell-Induced Differentiation. Cells were plated into a 12-well plate and cultured with a-MEM containing 100 μg/mL ascorbic acid, 10 mM B-glycerophosphate, 1% penicillin-streptomycin, and 10% FBS on the condition of 95% N2 and 5% CO_2 at 37°C. After different incubation times (1, 3, 7, 14, and 21 days), the cells were used for additional experiments.

2.3. Preparation of Solution and Conditioned Medium (CM). The preparation of osteogenic induction solution was performed as follows. β-sodium glycerophosphate solution (10 mM) and ascorbic acid solution (50 mg/L) were prepared with α-MEM medium. 1 mL 50 mg/L ascorbic acid solution and 9 mL β-sodium glycerophosphate solution (10 mM) were mixed and 100 times concentrated osteogenic induction solution was obtained. After filtering with 0.22 μm filtration, the solution was kept away from light at -20°C.

The preparation of high sugar solution was performed as follows. The glucose solution (25 mmol/L) was prepared with α-MEM. After filtering with 0.22 μm filtration, the solution was kept away from light at -20°C.

The preparation of palmitic acid (PA) solution was performed as follows. 0.0307 g PA was added to 3 mL NaOH (0.1 mol/L). After saponification for 30 min at 75°C water bath, the 40 mM PA saponification solution was obtained.

The preparation of undercarboxylated osteocalcin (ucOC) was performed as follows. The ucOC (1 μg/μL) was prepared with DMSO. The ucOC (1 μg/μL) was diluted with PBS when use.

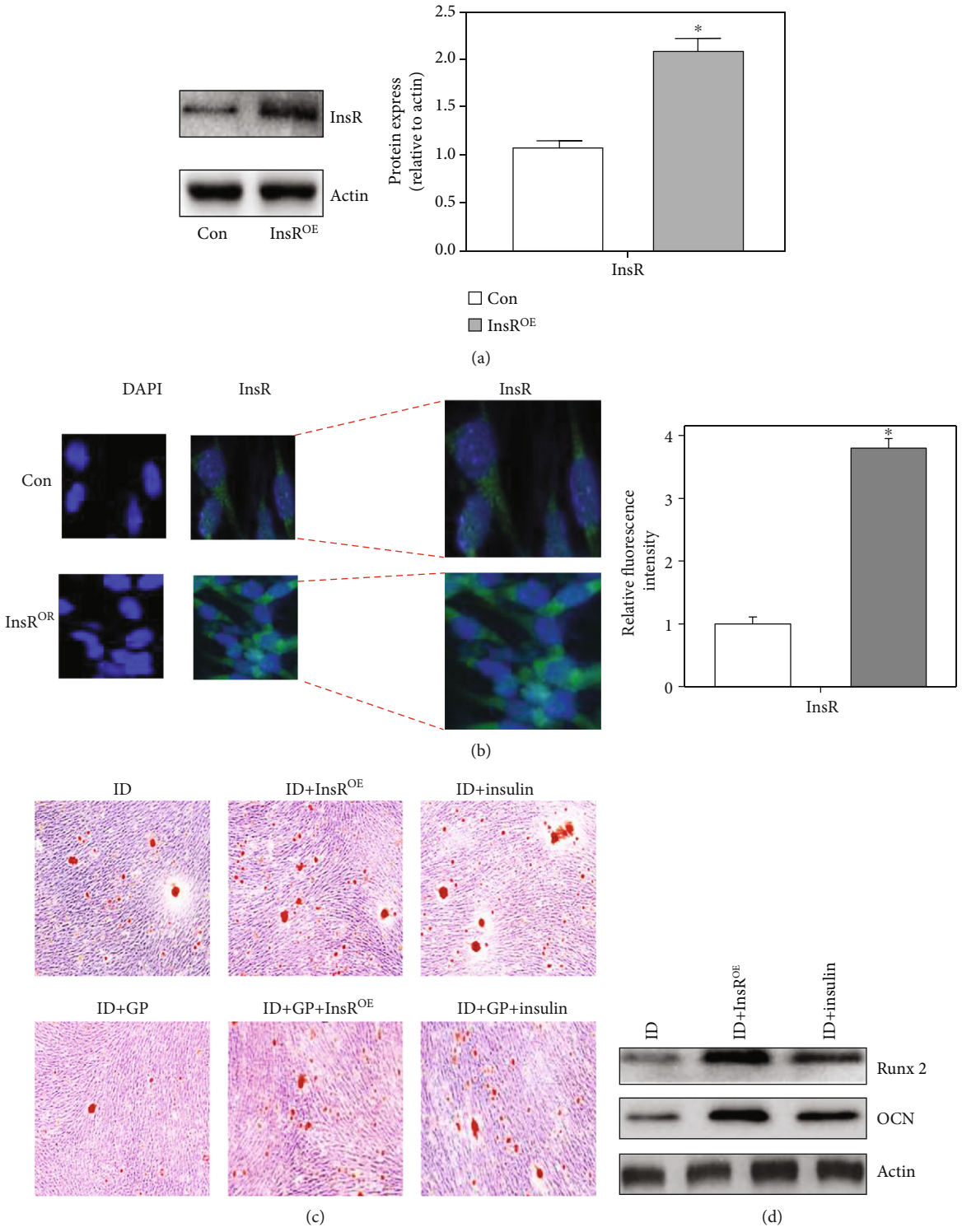

Figure 3: Continued.

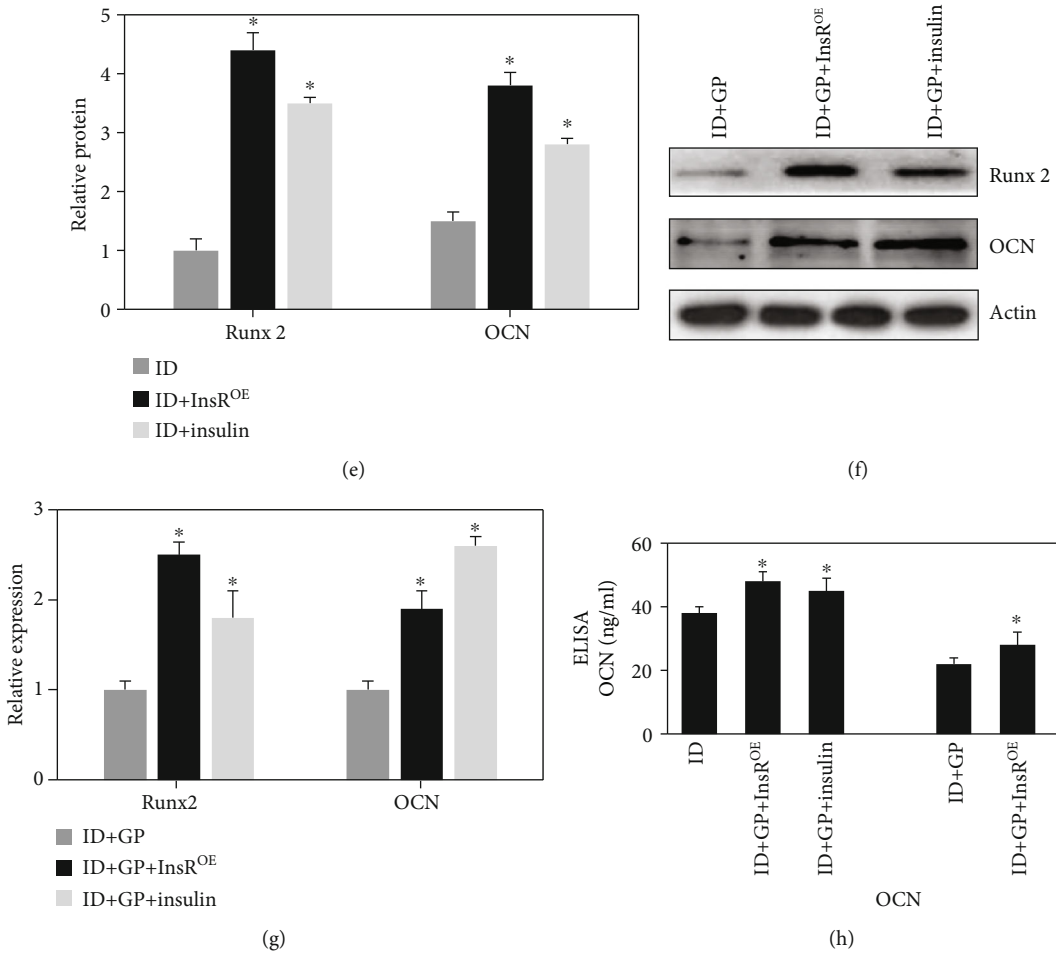

Figure 3: Effect of overexpression insulin receptor ($InsR^{OE}$) on Runx2 and OCN expression. (a) Establishment of insulin receptor overexpression model. (b) The establishment of insulin receptor overexpression model was validated through immunocytochemistry staining. (c) Mineralization was analyzed through alizarin red staining. (d) The protein expression of Runx2 and OCN was measured through western blotting after treatment with ID, ID+$InsR^{OE}$, or ID+Insulin. (e) The protein expression of Runx2 and OCN was analyzed. (f) The protein expression of Runx2 and OCN was measured through western blotting after treatment with ID+GP, ID+GP + $InsR^{OE}$, or ID+GP + Insulin. (h) The protein expression of Runx2 and OCN was analyzed. (g) The level of OCN was measured with ELISA. Compared with the ID or ID+GP group, $^*P < 0.05$. MC3T3-E1 was used in these experiments.

The preparation of CM was performed as follows. The $InsR^{OE}$ MC3TC-E1 cells were induced differentiation for 14 days. The CM was collected and centrifuged at 1500 g for 10 minutes. The supernatant was collected, filtered, and stored at -80°C for use.

2.4. Plasmid Construction and Transfection. The InsR ovexpression ($InsR^{OE}$) plasmid was constructed using pDC316-mCMV-EGFP. The primer was designed and synthesized by GenePharma (Shanghai, China). The cells were transfected with vector using transient transfection. The cells were subjected to further experimentation after transfection.

2.5. Flow Cytometric Measurement. Cells were seeded in a 6-well plate and cultured on the condition of 37°C and 5% CO_2. After treatment with PA (20 mM) or ucOC (1 μg/μL) for 4 h, the cells were digested using trypsin. After centrifugation at 8,000 rpm for 10 min, the cells were collected and suspended with cold PBS. Then, cells were incubated with propidium iodide and Annexin V-FITC for 30 min in the dark and analyzed using the Cytomics™ FC500 Flow Cytometer (Beckman, USA).

2.6. Immunofluorescence Analysis. β-TC6 cells were fixed using paraformaldehyde (4%) for 30 min and then incubated using 0.2% Triton X-100 (20 min). PBS containing 8% BSA was used for blocking. Cells were incubated with anti-FOXO1(1 : 500) or anti-TLR4 (1 : 800) overnight at 4°C. After washing twice with PBS, the cells were incubated with second antibody at room temperature for 1 h. DAPI was used to stain the nuclei for 5 min. A confocal microscope was used to analyze fluorescent images.

2.7. qRT-PCR. The total RNA was extracted from the β-TC6 cells with the TRIzol reagent (Invitrogen, USA). The reverse transcription was performed according to the previous report [29]. Reverse transcription product (2 μL) was mixed with 10.0 μL of qPCR SYBR® Green Master Mix (A6001,

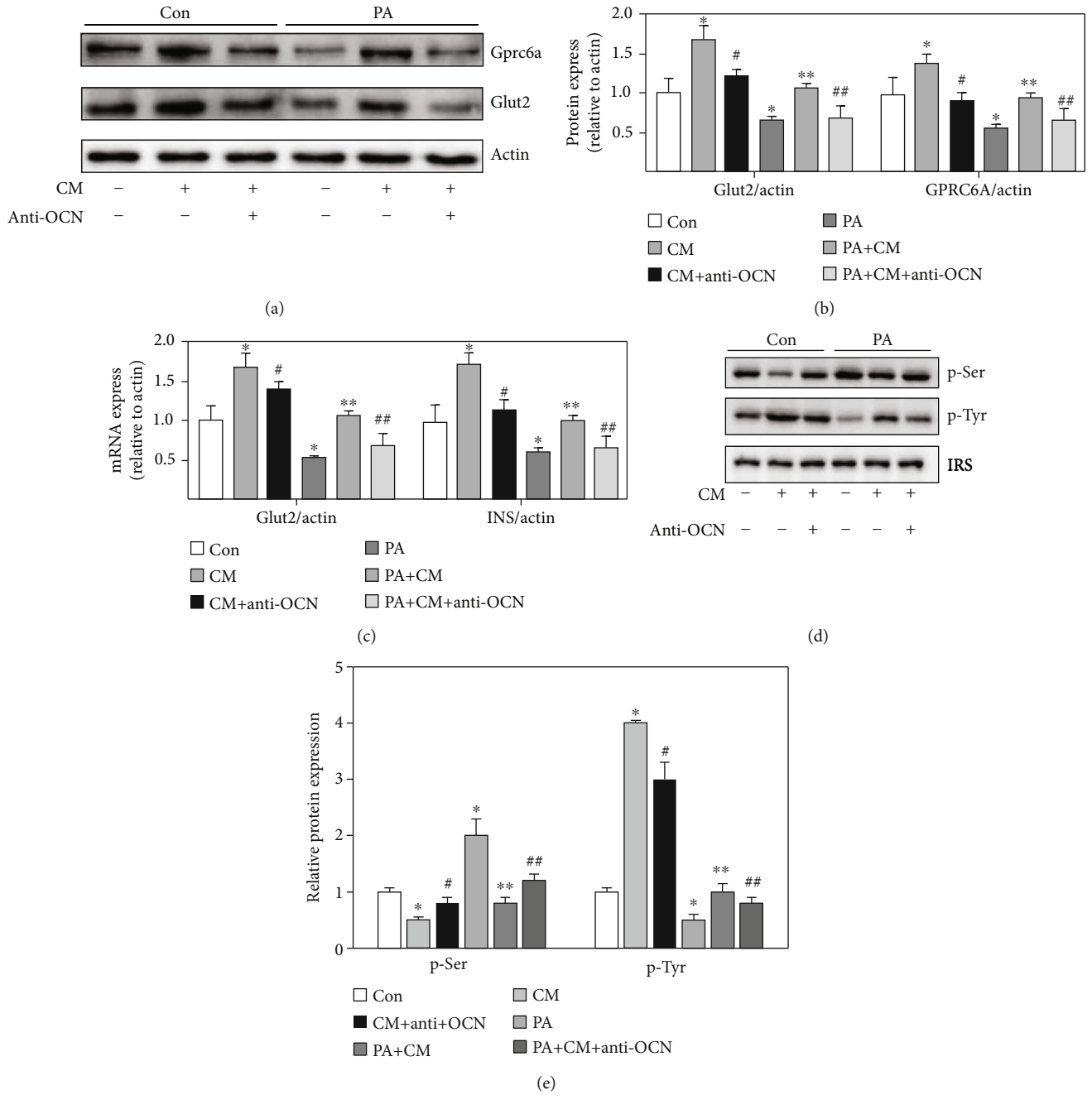

Figure 4: The increase of insulin by CM was reversed by Anti-OCN. (a) The protein expression of Gprc6a and Glut2 was measured through western blotting after treatment with CM or Anti-OCN. (b) The protein expression of Gprc6a and Glut2 was analyzed. (c) The mRNA expression of Gprc6a and Glut2 was measured through qRT-PCR after treatment with CM or Anti-OCN. (d) The serine and threonine phosphorylation of insulin receptor substrate 1 (IRS-1) were measured through western blotting after treatment with CM or Anti-OCN. (e) The serine and threonine phosphorylations of insulin receptor substrate 1 (IRS-1) were analyzed. Compared with the control group, $^{*}P < 0.05$. Compared with the PA group, $^{**}P < 0.05$. Compared with the CM group, $^{\#}P < 0.05$. Compared with the PA + CM group, $^{\#\#}P < 0.05$. Beta-TC6 was used in these experiments.

Promega, USA), 0.5 μL of primers, and 7.0 μL nuclease-free water. Subsequently, the ABI 7500 PCR system (ABI, USA) was used to detect the mRNA expression. The $2^{-\triangle\triangle Ct}$ method was used to calculate mRNA expression [30]. The primers were listed as follows: Runx2: F: 5′-ATGCTTCATTCGCCTCACAAA-3′, R: 5′-GCACTCACTGACTCGGTTGG-3′; OCN: F: 5′-CATGCCAGGTCACCAAAT-3′, R: 5′-GCCCCAAGGCCGCTTCTT-3′; Glut2: F: 5′-GAAGACAAGATCACCGGAACCTTGG-3′, R: 5′-GGTCATCCAGTGGAACACCCAAAA-3′; Insulin F: 5′CCCACCCAGGCTTTTGTCAAACAGC-3′, R: 5′-TCCAGCTGGTAGAGGGAGCAGATG-3′; Actin: F: 5′-AGAGCTACGAG

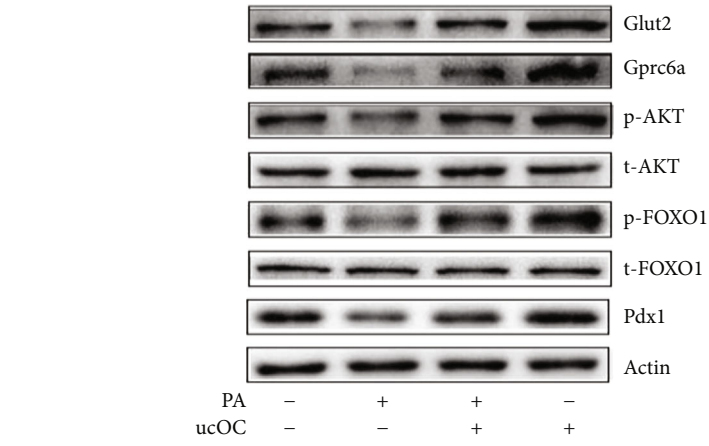

(a)

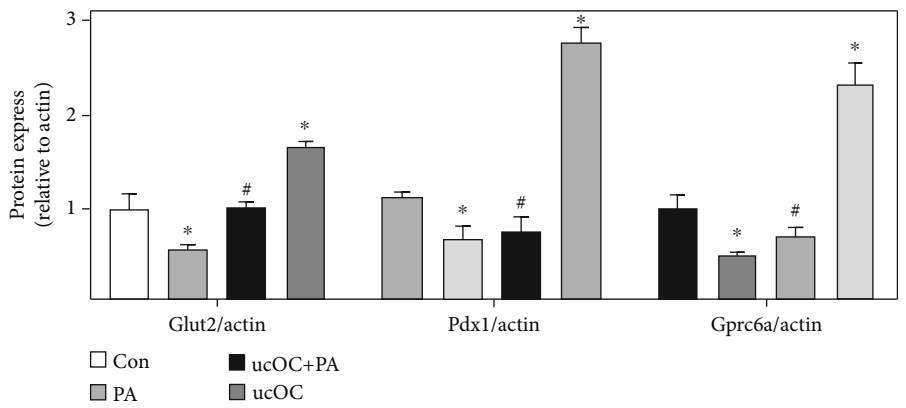

(b)

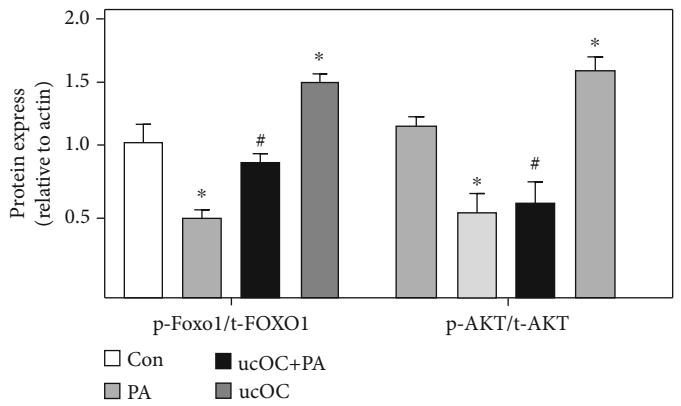

(c)

Figure 5: Continued.

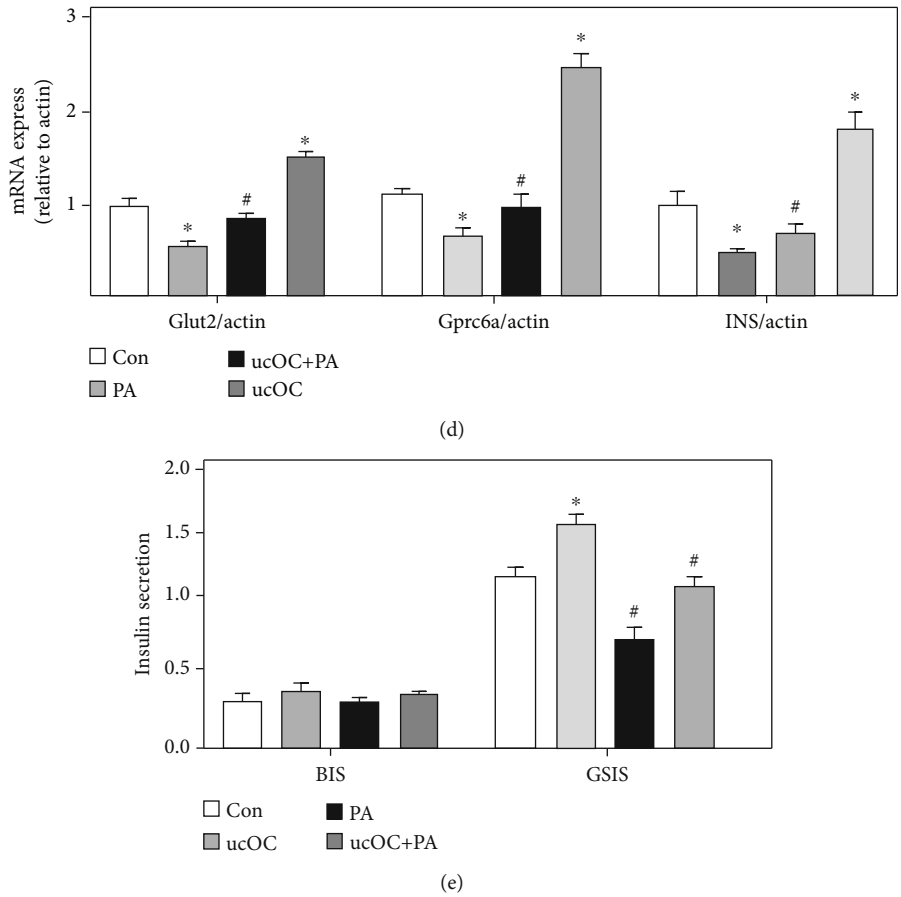

Figure 5: ucOC suppressed the lipotoxic islet β-cell damage caused by PA. (a) The protein expression of Gprc6a, Glut2, AKT, FOXO1, and Pdx1 was measured through western blotting after treatment with PA or ucOC. (b) The protein expression of Gprc6a and Glut2 was analyzed. (c) The protein expression of AKT and FOXO1 was analyzed. (d) The mRNA expression of Gprc6a and Glut2 was measured through qRT-PCR. (e) The insulin secretion was analyzed. Compared with the control group, $^{*}P < 0.05$. Compared with the PA group, $^{\#}P < 0.05$. Beta-TC6 was used in these experiments.

CTGCCTGAC-3′, R: 5′-AGCACTGTGTTGGCGTACAG-3′.

2.8. Western Blotting. The protein samples were extracted from the cells with RIPA buffer including the PMSF. The supernatant solution was collected after centrifuging at 8 000 rpm for 10 min. Same amounts of proteins were separated with SDS-PAGE. Then, the proteins were transferred to a PVDF membrane (Sigma, USA). After blocking with TBST, the membrane was incubated with anti-GLUC2, T-AKT, p-AKT, p-FOXO1, T-FOXO1, Pdx1, and β-actin (1 : 1500, Abcam, Beijing, China) overnight at 4°C. After washing twice, the membrane was incubated with secondary antibody (antimouse HRP-conjugated antibody, 1 : 2000) for 1 h. Finally, the protein was detected by chemiluminescence with Thermo ECL Substrate (Bio-Rad) and analyzed using the ImageJ software.

2.9. Alizarin Red Staining. The cells were fixed using paraformaldehyde (4%) for 20 min. After washing with water twice, the cells were stained using alizarin red staining solution (pH 4.2) for 20 min. After washing with water for 3 times, the cells were captured using a microscope.

2.10. TUNEL Staining. β-TC6 cells were fixed using paraformaldehyde (4%) for 30 min and washed with PBS. 0.2% Triton X-100 was used to incubate cell for 5 min. The TUNEL staining solution was prepared with TdT enzyme and fluorescent labeling solution (#C1090, Beyotime, Shanghai, China) according to the instruction. The cells were incubated with TUNEL staining solution in the dark at 37°C for 60 min. After washing 3 times with PBS, the cells were observed with a confocal microscope. DAPI was used to stain the nuclei for 3 min.

2.11. Statistical Analysis. Data was shown as mean ± SD and analyzed with the SPSS software (20.0, IBM, USA). Student's t-test or a one-way ANOVA were performed for data analysis. $P < 0.05$ was believed to be statistically different.

3. Results

3.1. Induction Time of Osteogenic Precursor Cells. β-Sodium glycerophosphate was used as an osteogenic inducer to induce osteoblast differentiation. Alizarin red staining showed that mineralization gradually increased with the extension of differentiation time, and more mineralized

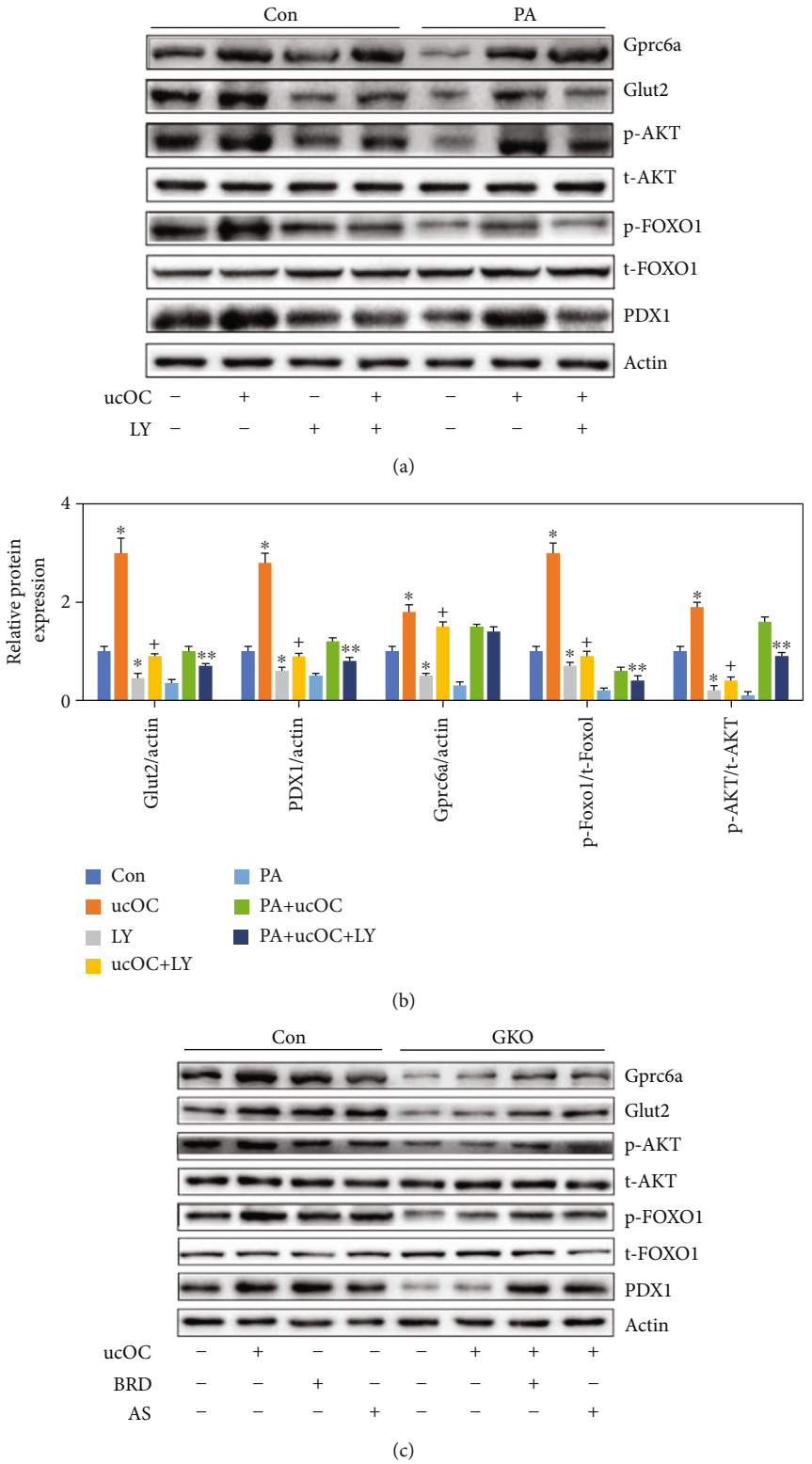

Figure 6: Continued.

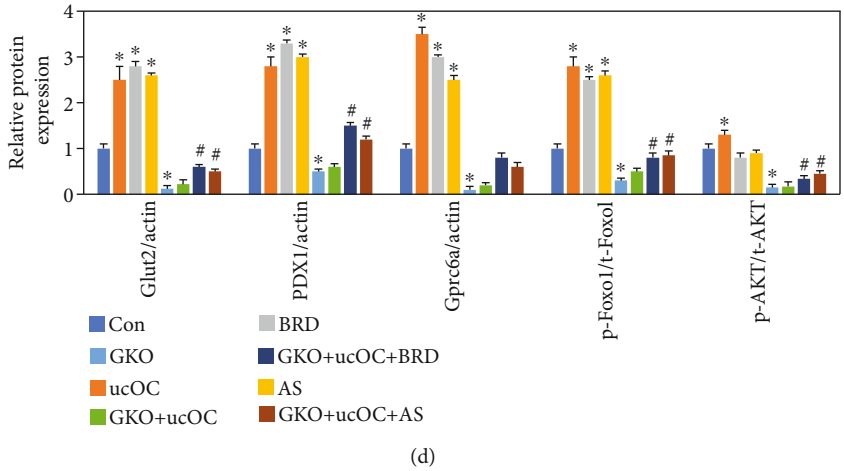

(d)

Figure 6: Knockdown of Gprc6a or suppression of PI3K/AKT signal pathway could reverse the upregulation of GPRC6A/PI3K/AKT/FoxO1/Pdx1 caused by ucOC. (a) The protein expression of Gprc6a, Glut2, AKT, FOXO1, and Pdx1 was measured through western blotting after treatment with PA, ucOC, and LY (the inhibitor of PI3K/AKT signal pathway). (b) The protein expression of Gprc6a, Glut2, AKT, FOXO1, and Pdx1 was analyzed. (c) The protein expression of Gprc6a, Glut2, AKT, FOXO1, and Pdx1 was measured through western blotting after treatment with ucOC, BRD (The inducer of Pdx1), and AS (The inhibitor of Foxi1). (d) The protein expression of Gprc6a, Glut2, AKT, FOXO1, and Pdx1 was analyzed. Compared with the control group, $^{*}P < 0.05$. Compared with the GKO + ucOC group, $^{\#}P < 0.05$. Compared with the ucOC group, $^{+}P < 0.05$. Compared with the PA + ucOC group, $^{**}P < 0.05$. Beta-TC6 was used in these experiments.

nodules were produced at 14 days of differentiation (Figure 1(a)). The protein and mRNA expression of Runx2 and OCN were increased gradually with the extension of differentiation time (Figures 1(b), 1(c), and 1(e)). The increase trend of OCN was also identified with ELISA method, and it was promoted with the increase of differentiation time (Figure 1(d)).

3.2. High-Glucose and High-Fat Diet Inhibited the Differentiation of Osteoblast Precursors. Based on the data in Figure 1, 14-day incubation was used for induction differentiation (ID). The high-glucose and high-fat model was established with glucose (25 mM) and palmitic acid (100 mM) (GP). We found that mineralized nodules were markedly decreased in the group ID+GP compared with the group ID (Figure 2(a)). In addition, the protein and mRNA levels of Runx2 and OCN were significantly decreased after GP treatment compared with ID administration only (Figures 2(b)–2(e)). Therefore, high-glucose and high-fat diet could inhibit the differentiation of osteoblast precursors.

3.3. Effect of Insulin Receptor Overexpression ($InsR^{OE}$) on Runx2 and OCN Expression. In order to verify the important role of insulin signaling pathway in the process of osteoblast differentiation, we overexpressed the insulin receptor of osteoblast precursor cells (MC3T3-E1). In addition, whether insulin stimulation can stimulate osteoblast differentiation and improve the obstacle of osteoblast differentiation caused by GP was also studied. The successful establishment of insulin receptor overexpression model in the osteoblast precursor cells was verified through western blotting (Figure 3(a)) and immunocytochemistry staining (Figure 3(b)). We found that the mineralized nodules were significantly increased in the group ID+$InsR^{OE}$ and ID+Insulin compared with the group ID (Figure 3(c)). Meanwhile, in the GP-treated model, both $InsR^{OE}$ and insulin significantly promoted the mineralized nodules number (Figure 3(c)). In addition, $InsR^{OE}$ and insulin increased remarkably the protein and mRNA levels of Runx2 and OCN in both ID- and ID+GP-treated models (Figures 3(d)–3(h)). Therefore, overexpression of InsR and insulin can increase the expression levels of osteogenic differentiation indexes including OCN and Runx2 and improve the obstacle of osteoblast differentiation caused by glycolipid toxicity.

3.4. The Insulin Increased by CM Overexpressing Insulin Receptor Was Reversed by Osteocalcin Neutralizing Antibody (Anti-OCN). The influences of CM and Anti-OCN on the expression of GSIS glucose transporters, Gprc6a, and Glut2, in the membrane of islet β-cell were investigated. We found that PA remarkably reduced the levels of Gprc6a, Glut2, and insulin compared with the group control (Figures 4(a)–4(c))In addition, the levels of Gprc6a, Glut2, and insulin were remarkably increased by CM, but the increased effects were suppressed by Anti-OCN (Figures 4(a)–4(c)). Therefore, the increase of Gprc6a and Glut2 by CM should be achieved by the OCN secreted by MC3TC-E1 cells overexpressing $InsR^{OE}$. After treatment with anti-OCN, the promotion of Gprc6a, Glut2, and insulin by CM was suppressed. OCN might affect GSIS and insulin through regulating insulin receptor. In addition, the activation of insulin signaling was investigated through measuring the serine and threonine phosphorylation of insulin receptor substrate 1 (IRS-1). We found that CM remarkably promoted threonine phosphorylation but decreased serine phosphorylation compared with the group control (Figures 4(d) and 4(e)). However, the influence of CM on the activation of insulin

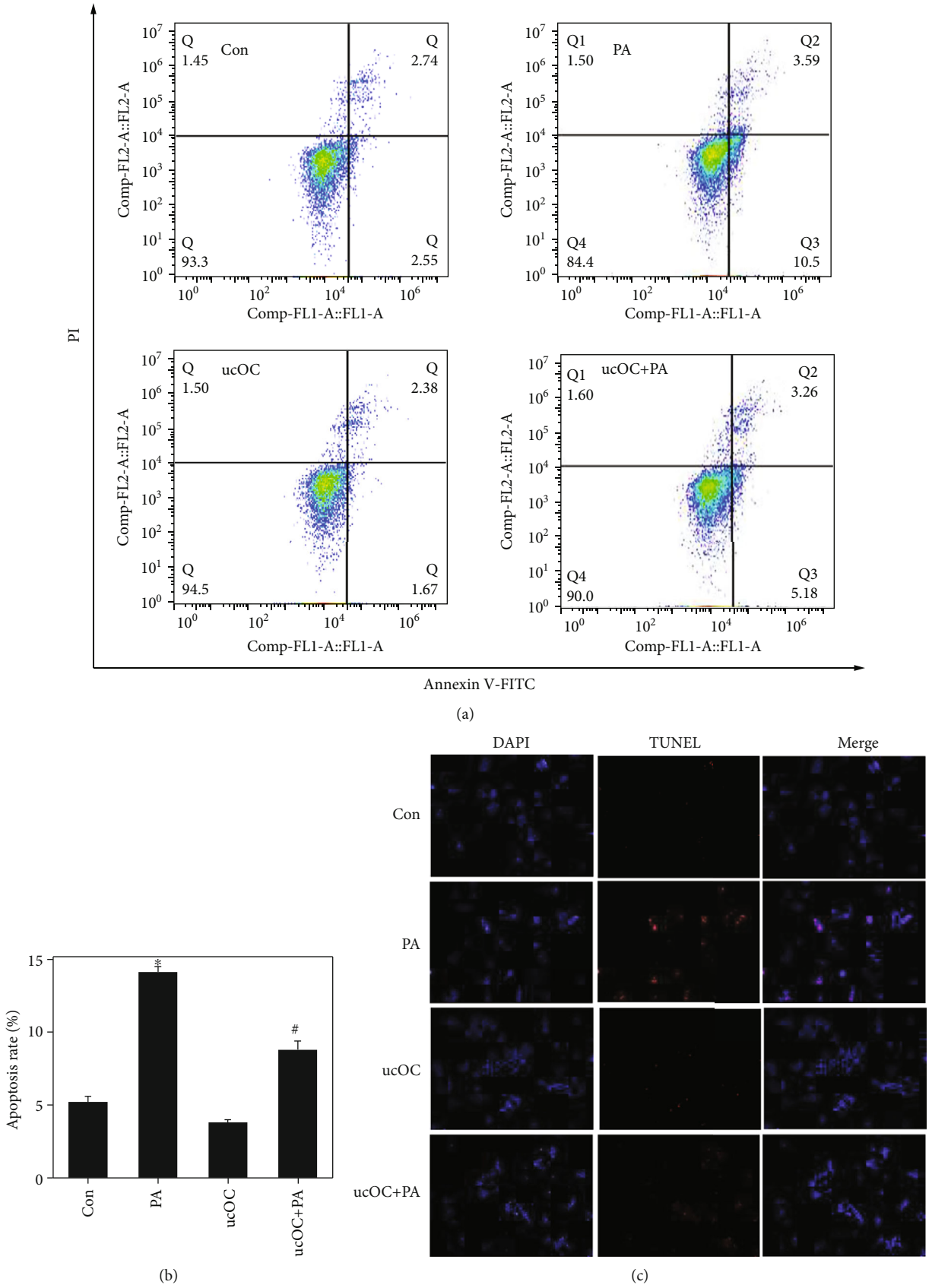

Figure 7: Continued.

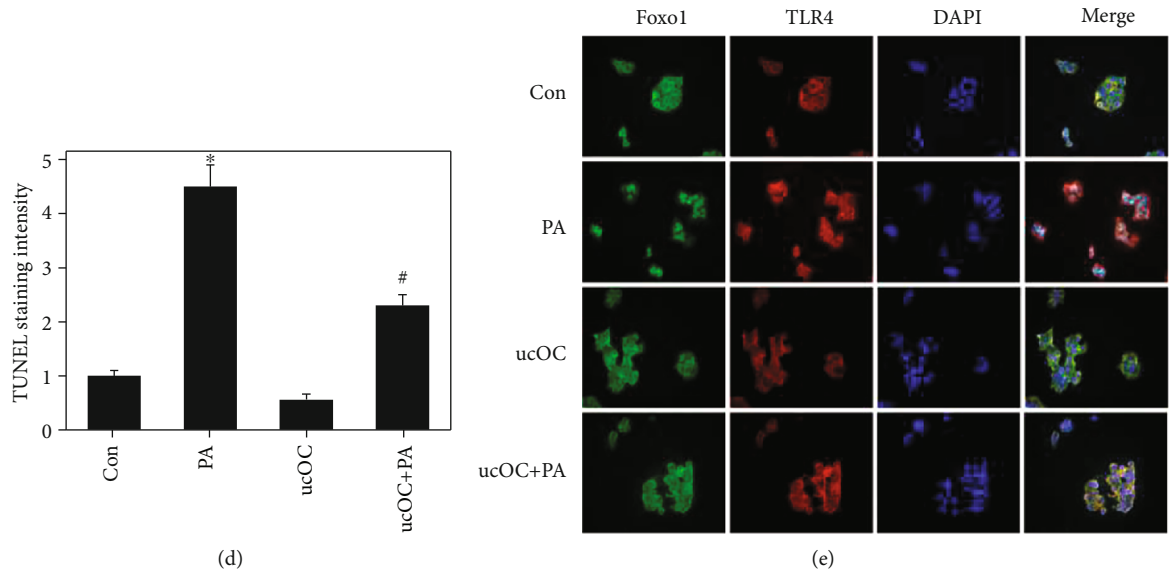

Figure 7: ucOC suppressed the apoptosis of islet β-cell and regulated FOXO1 nuclear transfer. (a) The cell apoptosis was measured after treatment with PA or ucOC. (b) The cell apoptosis was analyzed. (c) The cell apoptosis was measured with TUNEL staining. (d) The cell apoptosis was analyzed. (e) The FOXO1 nuclear transfer and TLR4 expression were measured after treatment with PA or ucOC. Beta-TC6 was used in these experiments.

signaling was reversed by anti-OCN (Figures 4(d) and 4(e)). Meanwhile, the decreased threonine phosphorylation and increased serine phosphorylation induced by PA were reversed by CM (Figures 4(d) and 4(e)).

3.5. Undercarboxylated Osteocalcin (ucOC) Suppressed the Lipotoxic Islet β-Cell Damage Caused by PA. The decreased levels of Glut2, Gprc6a, p-AKT/t-AKT, p-FOXO1/t-FOXO1, and Pdx1 caused by PA were significantly increased by ucOC (Figures 5(a)–5(c)). In addition, the results were identified through qRT-PCR (Figure 5(d)). Meanwhile, the decreased insulin secretion induced by PA was also promoted by ucOC (Figures 5(d) and 5(e)). Therefore, ucOC could activate AKT and FOXXO1 and improve insulin secretion disorder caused by lipotoxicity.

3.6. Knockdown of Gprc6a or Suppression of PI3K/AKT Signal Pathway Could Reverse the Upregulation of GPRC6A/PI3K/AKT/FoxO1/Pdx1 Caused by ucOC. LY294002 (LY) was used as the inhibitor of PI3K/AKT signal pathway in this study. We found that the levels of Glut2, Gprc6a, p-AKT/t-AKT, p-FOXO1/t-FOXO1, and Pdx1 were significantly inhibited after treatment with LY (Figures 6(a) and 6(b)). In addition, the Gprc6a gene was knocked down in the cells through transfection. After knockdown of Gprc6a, the increase of Glut2 induced by ucOC was blocked (Figures 6(c) and 6(d)), and the levels of Glut2, Gprc6a, p-AKT/t-AKT, p-FOXO1/t-FOXO1, and Pdx1 were significantly suppressed. After supplement with AS1842856 (AS, the inhibitor of Foxi1) or BRD7552 (BRD, the inducer of Pdx1), these inhibition effects were improved.

3.7. ucOC Suppressed the Apoptosis of Islet β-Cell and Regulated FOXO1 Nuclear Transfer. To explore the mechanism of how OCN suppresses glycolipid toxicity and improves insulin, cell apoptosis and FOXO1 nuclear transfer were analyzed. We found that apoptosis rate was significantly reduced from 14.09% in the group PA to 8.44% in the group ucOC+PA (Figures 7(a) and 7(b)). The cell apoptosis was also validated with TUNEL staining. The remarkable increase of cell apoptosis induced by PA was decreased by ucOC (Figures 7(c) and 7(d). Meanwhile, ucOC remarkably promoted the transfer of FOXO1 from intranuclear to extranuclear compared with the group PA and inhibited the expression of TLR4 (Figure 7(e)).

4. Discussion

Diabetes is a very common disease and it significantly threats people's health worldwide [1, 2, 31]. The metabolic disorder can be induced by high blood glucose levels or the insulin reduction in the diabetes patients [32]. The differentiation of mature β-cell was also an important factor in functional cell reduction and insulin secretion deficiency in patients with diabetes [9, 10]. Our previous studies suggest that chronic exposure to high concentrations of saturated fatty acids, such as palmitic acid (PA) and osteocalcin, could lead to apoptosis of pancreatic β-cells [11–13]. Osteocalcin is the bridge between bone metabolism and energy metabolism [14, 15]. Some researchers found that there was no abnormal bone metabolism after selective osteocalcin gene knockout in rats [16]. However, fat thickness, insulin level, glucose tolerance, and other metabolic indicators could be changed, and the real function of this protein has not been well understood [16, 20, 21]. We found that the level of insulin and the expression of GLUT2 were significantly increased in the OCN treatment group compared with the control. Especially, the secretion of insulin was obviously increased. After intervention with

exogenous OCN in mice fed with high fat and high glucose, the fat thickness of mice was decreased, but the insulin secretion and sensitivity were increased [22–25].

Previous evidence suggests that β-cell dysfunction during the development of T2DM could be regulated by the changes of insulin section [33, 34] and the increase of ceramide, nitric oxide, ROS, and mitochondrial perturbations [35–37]. Several studies have proved that a Fox family transcription factor was involved in the regulation of exocytosis-related gene expression in β-cells, especially FOXO1 [38–40]. FOXO1 is a target in the insulin pathway, inhibition of this pathway could reduce exocytotic gene and protein expression, resulting in the dysfunction of cells [39, 41, 42]. In our study, the result showed that the OCN treatment significantly increased the FOXO1 from intranuclear to extranuclear compared with the group PA. Our results are consistent with the view that FOXO1 plays an important role in the gradual decline of β-cell function [38]. The PDX1 protein was significantly increased after OCN treatment. The PDX1 protein was an important protein in dedifferentiated β-cell [43, 44]. The previous result also showed that the PDX1 expression was increased in islets of T2DM [44]. Based on the above discussion, our results suggest that OCN was an important protein regulating the GLUT2 and PDX1 protein expression in the β-TC6 cell.

In summary, our data demonstrated that OCN improved lipotoxic inflammation and apoptosis in β-TC6 cells by upregulating the GLUT2 expression and activating FOXO1 pathway. Our results suggested that OCN could activate the FOXO1 signaling pathway to regulate GLUT2 expression and improve the insulin secretion disorder caused by lipotoxicity.

Abbreviations

OCN: Osteocalcin
T2DM: Type 2 diabetes mellitus
$InsR^{OE}$: Overexpression of insulin receptor
ucOC: Undercarboxylated osteocalcin
PA: Palmitic acid
CM: Osteoblast culture medium overexpressing insulin receptor
ID: Induction differentiation
GP: Glucose and palmitic acid
Anti-OCN: Osteocalcin neutralizing antibody
AS: AS1842856
BRD: BRD7552
LY: LY294002.

Data Availability

Data supporting this study has been presented in the manuscript, the data required by editor, reviewer, and reader could be provided by the corresponding author.

Ethical Approval

The study has been approved by the Ethics Committee of Fujian Medical University,

Consent

All authors agree to the publication of this manuscript.

Conflicts of Interest

The authors declare that they have no conflict of interest.

Authors' Contributions

LH conceived and designed the experiments; YZ, LL, YZ, and SY performed the experiments; and HL wrote the paper.

Acknowledgments

This study was supported by Natural Science Foundation of Fujian Province (2018 J01171).

References

[1] L. Cordain, S. B. Eaton, A. Sebastian et al., "Origins and evolution of the Western diet: health implications for the 21st century," *The American Journal of Clinical Nutrition*, vol. 81, no. 2, pp. 341–354, 2005.

[2] B. Y. Kim, J. C. Won, J. H. Lee et al., "Diabetes fact sheets in Korea, 2018: an appraisal of current status," *Diabetes & Metabolism Journal*, vol. 43, no. 4, pp. 487–494, 2019.

[3] S. Bhattacharya, P. Manna, R. Gachhui, and P. C. Sil, "D-saccharic acid-1,4-lactone ameliorates alloxan-induced diabetes mellitus and oxidative stress in rats through inhibiting pancreatic beta-cells from apoptosis via mitochondrial dependent pathway," *Toxicology and Applied Pharmacology*, vol. 257, no. 2, pp. 272–283, 2011.

[4] N. Irwin, V. A. Gault, F. P. M. O'Harte, and P. R. Flatt, "Blockade of gastric inhibitory polypeptide (GIP) action as a novel means of countering insulin resistance in the treatment of obesity-diabetes," *Peptides*, vol. 125, article 170203, 2020.

[5] M. P. Czech, "Insulin action and resistance in obesity and type 2 diabetes," *Nature Medicine*, vol. 23, no. 7, pp. 804–814, 2017.

[6] R. B. Sharma and L. C. Alonso, "Lipotoxicity in the pancreatic beta cell: not just survival and function, but proliferation as well?," *Current Diabetes Reports*, vol. 14, no. 6, p. 492, 2014.

[7] J. Veret, L. Bellini, P. Giussani, C. Ng, C. Magnan, and H. Le Stunff, "Roles of sphingolipid metabolism in pancreatic β cell dysfunction induced by lipotoxicity," *Journal of Clinical Medicine*, vol. 3, no. 2, pp. 646–662, 2014.

[8] X. Shen, L. Yang, S. Yan et al., "Fetuin A promotes lipotoxicity in β cells through the TLR4 signaling pathway and the role of pioglitazone in anti-lipotoxicity," *Molecular and Cellular Endocrinology*, vol. 412, pp. 1–11, 2015.

[9] S. Del Guerra, R. Lupi, L. Marselli et al., "Functional and molecular defects of pancreatic islets in human type 2 diabetes," *Diabetes*, vol. 54, no. 3, pp. 727–735, 2005.

[10] R. Lupi, S. Del Guerra, R. Mancarella et al., "Un nouveau scavenger des especes reactives de l'oxygene corrige *in vitro* les defauts de la secretion d'insuline des ilots diabetiques humains de type 2," *Diabetes & Metabolism*, vol. 33, no. 5, pp. 340–345, 2007.

[11] J. N. Xiang, D. L. Chen, and L. Y. Yang, "Effect of PANDER in βTC6-cell lipoapoptosis and the protective role of exendin-4," *Biochemical and Biophysical Research Communications*, vol. 421, no. 4, pp. 701–706, 2012.

[12] D. L. Chen, J. N. Xiang, and L. Y. Yang, "Role of ERp46 in β-cell lipoapoptosis through endoplasmic reticulum stress pathway as well as the protective effect of exendin-4," *Biochemical and Biophysical Research Communications*, vol. 426, no. 3, pp. 324–329, 2012.

[13] N. Dirckx, M. C. Moorer, T. L. Clemens, and R. C. Riddle, "The role of osteoblasts in energy homeostasis," *Nature Reviews Endocrinology*, vol. 15, no. 11, pp. 651–665, 2019.

[14] T. Shimizu, M. Takahata, Y. Kameda et al., "Vitamin K-dependent carboxylation of osteocalcin affects the efficacy of teriparatide ($PTH_{1\text{-}34}$) for skeletal repair," *Bone*, vol. 64, pp. 95–101, 2014.

[15] C. M. Gundberg, J. B. Lian, and S. L. Booth, "Vitamin K-dependent carboxylation of osteocalcin: friend or foe?," *Advances in Nutrition*, vol. 3, no. 2, pp. 149–157, 2012.

[16] L. J. Lambert, A. K. Challa, A. Niu et al., "Increased trabecular bone and improved biomechanics in an osteocalcin-null rat model created by CRISPR/Cas 9 technology," *Disease Models & Mechanisms*, vol. 9, no. 10, pp. 1169–1179, 2016.

[17] M. Rauner, U. Foger-Samwald, M. F. Kurz et al., "Cathepsin S controls adipocytic and osteoblastic differentiation, bone turnover, and bone microarchitecture," *Bone*, vol. 64, pp. 281–287, 2014.

[18] Y. Xiong, Y. Zhang, N. Xin et al., "1α,25-Dihydroxyvitamin D_3 promotes bone formation by promoting nuclear exclusion of the FoxO1 transcription factor in diabetic mice," *The Journal of Biological Chemistry*, vol. 292, no. 49, pp. 20270–20280, 2017.

[19] M. Kaneki, "Is ucOC a novel bone-derived anti-diabetogenic hormone in humans?," *Clinical Calcium*, vol. 19, no. 9, pp. 1304–1310, 2009.

[20] N. K. Lee, H. Sowa, E. Hinoi et al., "Endocrine regulation of energy metabolism by the skeleton," *Cell*, vol. 130, no. 3, pp. 456–469, 2007.

[21] X. Lin, L. Parker, E. McLennan et al., "Uncarboxylated osteocalcin enhances glucose uptake ex vivo in insulin-stimulated mouse oxidative but not glycolytic muscle," *Calcified Tissue International*, vol. 103, no. 2, pp. 198–205, 2018.

[22] X. Lin, L. Parker, E. McLennan et al., "Undercarboxylated osteocalcin improves insulin-stimulated glucose uptake in muscles of corticosterone-treated mice," *Journal of Bone and Mineral Research: the Official Journal of the American Society for Bone and Mineral Research*, vol. 34, no. 8, pp. 1517–1530, 2019.

[23] A. Pandey, H. R. Khan, N. S. Alex, M. Puttaraju, T. T. Chandrasekaran, and M. Rudraiah, "Under-carboxylated osteocalcin regulates glucose and lipid metabolism during pregnancy and lactation in rats," *Journal of Endocrinological Investigation*, vol. 43, no. 8, pp. 1081–1095, 2020.

[24] X. L. Zhang, Y. N. Wang, L. Y. Ma, Z. S. Liu, F. Ye, and J. H. Yang, "Uncarboxylated osteocalcin ameliorates hepatic glucose and lipid metabolism in KKAy mice via activating insulin signaling pathway," *Acta Pharmacologica Sinica*, vol. 41, no. 3, pp. 383–393, 2020.

[25] X. L. Wu, X. Y. Zou, M. Zhang et al., "Osteocalcin prevents insulin resistance, hepatic inflammation, and activates autophagy associated with high-fat diet-induced fatty liver hemorrhagic syndrome in aged laying hens," *Poultry Science*, vol. 100, no. 1, pp. 73–83, 2021.

[26] L. Huang, L. Yang, L. Luo, P. Wu, and S. Yan, "Osteocalcin improves metabolic profiles, body composition and arterial stiffening in an induced diabetic rat model," *Experimental and Clinical Endocrinology & Diabetes*, vol. 125, no. 4, pp. 234–240, 2017.

[27] F. L. Bilotta, B. Arcidiacono, S. Messineo et al., "Insulin and osteocalcin: further evidence for a mutual cross-talk," *Endocrine*, vol. 59, no. 3, pp. 622–632, 2018.

[28] J. Wang, D. D. Yan, X. H. Hou et al., "Association of bone turnover markers with glucose metabolism in Chinese population," *Acta Pharmacologica Sinica*, vol. 38, no. 12, pp. 1611–1617, 2017.

[29] F. Qin, Z. Song, M. Chang, Y. Song, H. Frierson, and H. Li, "Recurrent cis-SAGe chimeric RNA, *D2HGDH-GAL3ST2* , in prostate cancer," *Cancer Letters*, vol. 380, no. 1, pp. 39–46, 2016.

[30] Z. Xie, J. Zhang, S. Ma, X. Huang, and Y. Huang, "Effect of Chinese herbal medicine treatment on plasma lipid profile and hepatic lipid metabolism in Hetian broiler," *Poultry Science*, vol. 96, no. 6, pp. 1918–1924, 2017.

[31] S. R. Whitworth, D. G. Bruce, S. E. Starkstein et al., "Risk factors and outcomes of anxiety symptom trajectories in type 2 diabetes: the Fremantle Diabetes Study Phase II," *Diabetic medicine: A Journal of the British Diabetic Association.*, vol. 37, no. 10, pp. 1688–1695, 2020.

[32] K. Maedler, J. Oberholzer, P. Bucher, G. A. Spinas, and M. Y. Donath, "Monounsaturated fatty acids prevent the deleterious effects of palmitate and high glucose on human pancreatic beta-cell turnover and function," *Diabetes*, vol. 52, no. 3, pp. 726–733, 2003.

[33] Y. W. Kim, J. S. Moon, Y. J. Seo et al., "Inhibition of fatty acid translocase cluster determinant 36 (CD36), stimulated by hyperglycemia, prevents glucotoxicity in INS-1 cells," *Biochemical and Biophysical Research Communications*, vol. 420, no. 2, pp. 462–466, 2012.

[34] J. H. Xue, Z. Yuan, Y. Wu et al., "High glucose promotes intracellular lipid accumulation in vascular smooth muscle cells by impairing cholesterol influx and efflux balance," *Cardiovascular Research*, vol. 86, no. 1, pp. 141–150, 2010.

[35] M. Shimabukuro, M. Ohneda, Y. Lee, and R. H. Unger, "Role of nitric oxide in obesity-induced beta cell disease," *The Journal of Clinical Investigation*, vol. 100, no. 2, pp. 290–295, 1997.

[36] I. Maestre, J. Jordan, S. Calvo et al., "Mitochondrial dysfunction is involved in apoptosis induced by serum withdrawal and fatty acids in the beta-cell line INS-1," *Endocrinology*, vol. 144, no. 1, pp. 335–345, 2003.

[37] P. A. Gerber and G. A. Rutter, "The role of oxidative stress and hypoxia in pancreatic beta-cell dysfunction in diabetes mellitus," *Antioxidants & Redox Signaling*, vol. 26, no. 10, pp. 501–518, 2017.

[38] M. Nagao, J. L. S. Esguerra, A. Asai et al., "Potential protection against type 2 diabetes in obesity through lower CD36 expression and improved exocytosis in β-cells," *Diabetes*, vol. 69, no. 6, pp. 1193–1205, 2020.

[39] K. Kaneko, K. Ueki, N. Takahashi et al., "Class IA phosphatidylinositol 3-kinase in pancreatic β cells controls insulin secretion by multiple mechanisms," *Cell Metabolism*, vol. 12, no. 6, pp. 619–632, 2010.

[40] N. Gao, P. White, N. Doliba, M. L. Golson, F. M. Matschinsky, and K. H. Kaestner, "Foxa2 controls vesicle docking and insulin secretion in mature β cells," *Cell Metabolism*, vol. 6, no. 4, pp. 267–279, 2007.

[41] K. K. Cheng, K. S. Lam, D. Wu et al., "APPL1 potentiates insulin secretion in pancreatic cells by enhancing protein kinase

Akt-dependent expression of SNARE proteins in mice," *Proceedings of the National Academy of Sciences of the United States of America*, vol. 109, no. 23, pp. 8919–8924, 2012.

[42] X. Wang, H. Gao, W. Wu et al., "The zinc transporter Slc39a5 controls glucose sensing and insulin secretion in pancreatic β-cells via Sirt1- and Pgc-1α-mediated regulation of Glut2," *Protein & Cell*, vol. 10, no. 6, pp. 436–449, 2019.

[43] Y. Kawaguchi, "Sox 9 and programming of liver and pancreatic progenitors," *The Journal of Clinical Investigation*, vol. 123, no. 5, pp. 1881–1886, 2013.

[44] M. Diedisheim, M. Oshima, O. Albagli et al., "Modeling human pancreatic beta cell dedifferentiation," *Molecular metabolism*, vol. 10, pp. 74–86, 2018.